vibrational spectrum has recently been questioned.[22]

The vibrational frequencies of $^3B_1$ and $^1B_1$ dimethylsilylene are listed in Table V. One interesting feature of these is the intensity pattern for the two modes occurring near 1400 cm^{-1} which, by analogy with $^1A_1$, should be observed experimentally near 1200 cm^{-1}. In $^1A_1$ these were both observable with moderate to strong intensity; for $^3B_1$ they are predicted to both be very weak, and for $^1B_1$ only the lower mode has appreciable intensity. Another striking feature is that the out-of-plane CH_3 rocking modes ν_{10} and ν_{14} have been shifted up several hundred wavenumbers. Finally, we note that the symmetric and asymmetric Si-C stretches, ν_6 and ν_{21}, are now split by about 100 cm^{-1} instead of being nearly degenerate. We hope these data will be of use to experimentalists.

Finally, to determine whether the species observed by Griller and co-workers[27,28] could possibly be the triplet state of dimethylsilylene, we have determined CISD-Q energies of various triplet states at the $^3B_1$ optimized geometry with the DZ+d basis set. Specifically, we have examined the $^3A_2$, $^3A_1$, and $^3B_2$ states which arise from the configurations $5b_2^2 8a_1^2 3b_1$ ($^3A_2$), $5b_2^2 8a_1 9a_1$ ($^3A_1$), and $5b_2^2 8a_1 6b_2$ ($^3B_1$). These states are analogous to the lowest energy triplet states of SiH_2 found by Rice and Handy.[13] The energy of $^3A_2$ is 127.5, 116.0, and 111.4 kcal/mol above $^3B_1$ at the SCF, CISD, and CISD-Q levels of theory, respectively. The corresponding values for $^3A_1$ are 128.5, 119.7, and 116.7 kcal/mol, and for $^3B_2$ we find 115.3, 113.3, and 112.3 kcal/mol. Thus we predict that excitations from $^3B_1$ to these higher lying triplets lie approximately 15-20 kcal/mol above the highest energy transitions observed by Griller (300 nm = 95.3 kcal/mol). While this suggests that the species observed by Griller is not $^3B_1$ dimethylsilylene, it is possible that larger basis sets and more highly correlated wave functions could reduce the splitting significantly.[13] Of course, the minima on the excited triplet state surfaces will be below the vertical excitation energies given above. Our results, in this regard, are therefore inconclusive.

Conclusions

The first excited $^3B_1$ and $^1B_1$ states of dimethylsilylene are predicted to lie 25 and 54 kcal/mol above the ground state, respectively. We find a vertical excitation energy of 63 kcal/mol for the $^1A_1$-$^1B_1$ transition. This agrees very well with the spectroscopic observations of West, Michl, and co-workers who find the absorption maximum at 450 nm (62.7 kcal/mol = 456 nm). Thus we concur that the species observed by these researchers is due to ground-state dimethylsilylene and that the recent objections of Griller and co-workers to the earlier spectroscopic assignment are unfounded.

Acknowledgment. We thank Prof. J. Michl for sending us a preprint of their latest results prior to publication. This research was supported by the Director, Office of Energy Research, Office of Basic Energy Sciences, Chemical Sciences Division of the U.S. Department of Energy under Contract Number DE-AC03-76SF00098. The Berkeley theoretical chemistry minicomputer is supported by the U.S. National Science Foundation (Grant CHE-8218785).

Registry No. $Si(CH_3)_2$, 6376-86-9.

Donor-Acceptor Interaction and the Peculiar Structures of Dications

Wolfram Koch,[1a] Gernot Frenking,*[1a] Jürgen Gauss,[1b] and Dieter Cremer*[1b]

Contribution from the Institut für Organische Chemie, Technische Universität Berlin, D-1000 Berlin 12, West Germany, and the Institut für Organische Chemie, Universität Köln, D-5000 Köln 41, West Germany. *Received March 10, 1986*

Abstract: The geometries and stabilities of dications are explained by the donor-acceptor interaction of a (neutral) donor and an (doubly charged) acceptor molecule, respectively. The bonding in these donor-acceptor complexes is analyzed by means of one-electron density analysis. A simple model is presented to rationalize the bonding features of dications CH_2X^{2+} and CH_4X^{2+}. Depending on the type and number of donor molecules, three cases of donor-acceptor complexes can be distinguished. Type I complexes comprise dications where the electron acceptor CH_2^{2+} is bound to molecule X which donates electronic charge via a lone-pair orbital. The second class (type II complexes) consists of species where electron donation of X arises from a bonding σ-MO, and type III complexes occur when two donor molecules, such as H_2 and X in CH_4X^{2+}, donate electronic charge into CH_2^{2+}. It is found that the geometries and stabilities of the three classes of dications can be explained by the strength and type of orbital interaction between donor and acceptor, respectively. The stabilization due to electron donation from two donors X and H_2 in type III dications is not simply additive but rather depends on the actual orbitals being involved in the interaction. The model presented here can be used to predict stable structures for unknown dications.

I. Introduction

In the last couple of years the experimental and theoretical study of doubly charged cations has become a very active field of chemical and physical research reflected in recent reviews on dications in solution[2] and in the gas phase.[3] Although doubly charged cations have been known since 1930,[4] only in the last 10 years has this field become a topic of broad interest. This is largely due to the development of new experimental techniques in gas-phase ion chemistry such as charge-stripping mass spectrometry, PIPICO (photoion-photoion coincidence), and IKES (ion kinetic energy spectroscopy), to mention only a few in this rapidly developing field. In solution, the use of superacids and "magic acids" facilitates the investigation of dications.[2] The interest in dications also arises from the finding that they exhibit some highly unusual structures: doubly charged methane is planar,[5] ethylene dication

(1) (a) Technische Universität Berlin. (b) Universität Köln.

(2) Surya Prakash, G. K.; Rawdah, T. N.; Olah, G. A. *Angew. Chem.* **1983**, *95*, 356.

(3) (a) Ast, T. *Adv. Mass Spectrom.* **1980**, *8A*, 555. (b) Schleyer, P. v. R. Division of Petroleum Chemistry, American Chemical Society, 1983, Vol. 28, p 4313. (c) Koch, W.; Maquin, F.; Stahl, D.; Schwarz, H. *Chimia* **1985**, *39*, 376. (d) Schleyer, P. v. R. Proceedings of the International Mass Spectrometry Congress, Swansea, 1985.

(4) Conrad, R. *Phys. Z.* **1930**, *31*, 888.

(5) (a) Collins, J. B.; Schleyer, P. v. R.; Binkley, J. B.; Pople, J. A. *J. Am. Chem. Soc.* **1976**, *98*, 3436. (b) Pople, J. A.; Tidor, B.; Schleyer, P. v. R. *Chem. Phys. Lett.* **1982**, *88*, 533. (c) Siegbahn, P. E. M. *Chem. Phys.* **1982**, *66*, 443.

0002-7863/86/1508-5808$01.50/0

has a perpendicular (D_{2d}) structure,[6] and the global minimum structure for a dication is often qualitatively different compared to the respective neutral species.[7] Dications (or higher charged species) may involve strongly bound helium and neon,[3d,8] and the removal of two π-electrons formally turns benzene into a Hückel antiaromate,[9] while cyclobutadiene dication can be considered as 2π aromate.[10] Pentacoordinate and even hexacoordinate carbon are found in dications which have been investigated in solution.[11] Thus, dications exhibit a fascinating new field in chemistry.

Contrary to neutral molecules, the prediction of a stable structure for a given formula of a dication has, in general, been a difficult problem. For example, the geometry corresponding to methanol(2+) is not even a minimum on the CH_4O^{2+} potential energy hypersurface.[7e] In a theoretical investigation on ethane dication by Olah and Simonetta[7a] the global minimum for $C_2H_6^{2+}$ was missed,[7b,12a] and a rather thorough study by Koch et al.[7c] on $C_2H_4O^{2+}$ species overlooked an unusual but energetically very low-lying structure which was later introduced by Lammertsma.[7d] In both cases, structures were missed which have a common feature in that they can be considered as composed from a smaller dicationic acceptor molecule (CH_4^{2+}) and a donor species (CH_2 and CO, respectively).

Donor–acceptor interaction has already been recognized as a stabilization for monocations in a class of structures called ion/dipole complexes[13] or ylide structures.[14] They can be described as structures with a strong bond between an electronegative atom, i.e., the negative charge center of a dipole, and the cationic center of a radical cation. Experimentally many ylide cations are well-known, among them $CH_2FH^{\bullet+}$,[15] $CH_2OH_2^{\bullet+}$,[16] and $CH_2NH_3^{\bullet+}$.[17] While these structures are not important for the neutral molecules, they often represent the global minimum on the potential energy surface of the respective radical cations.[14] Koch and Frenking[18] have shown that the stabilities of ylide cations can be explained by the donor–acceptor interaction of the constituting subunits, and they provided a model which predicts the existence and stability of hitherto unknown radical cations. Lammertsma[7d] has shown independently that a new class of dications, cation substituted methonium ions, can be explained in the same way as Koch and Frenking rationalized the ion/dipole complexes.[18]

This paper reports a similar but greatly extended analysis of donor–acceptor interaction, which is found to be even more important in dications compared to the singly charged cations. While ylide monocations exist as isomers besides classical structures, and both of them are often found experimentally as isomeric species separated by a substantial barrier to rearrangement,[15-18] dications with a classical structure are often not even a minimum on the potential energy surface but rearrange to the ylide dication.[14] For example, charge-stripping experiments do not reveal any evidence for a methanol dication, but rather the methyleneoxonium dication $CH_2OH_2^{2+}$ was detected[19] in perfect agreement with theoretical predictions.[7e] It will be shown that the unusual structures which were reported for many dications and overlooked in the case of $C_2H_6^{2+}$ [7a] and $C_2H_4O^{2+}$ [7c] could have easily been predicted with the principles which are presented here.

We present a simple model to rationalize the peculiar geometries, structures, and bonding features of dications CH_2X^{2+} and CH_4X^{2+} (X = FH, OH_2, NH_3, N_2, F_2, H_2, CO, OC, CH_2 ($^1A_1$), CH_4). This model is based upon the idea that the stabilities, geometries, and electronic structures of the CH_2X^{2+} and CH_4^{2+} dications can be explained by the interaction of a neutral donor molecule X and a dicationic acceptor CH_2^{2+} or CH_4^{2+}, respectively. Thus, the CH_2X^{2+} and CH_4^{2+} dications are considered as donor–acceptor complexes.[20] In the course of our investigation of CH_2X^{2+} and CH_4X^{2+} structures we found that we can distinguish between three classes of compounds. The first comprises dications CH_2X^{2+}, X = FH, OH_2, NH_3, N_2, CO, OC, CH_2 ($^1A_1$) (type I complexes), where the electron acceptor CH_2^{2+} is bound to a closed-shell molecule X which donates electronic charge by a lone-pair orbital n.

The second class comprises dications $CH_2Y_2^{2+}$ (type II complexes) with either Y_2 or H_2 donating electrons to CH_2^{2+} or CY_2^{2+} via a bonding σ MO ($\sigma(H_2)$ or $\sigma(Y_2)$) rather than a lone-pair orbital. In this work only two examples are discussed, namely $Y_2 = H_2$ and F_2.

Dications of the third class are formed by the interaction of *two* neutral donor molecules X and Y_2 with the dication CH_2^{2+}:

$$CH_2X(Y_2)^{2+}$$
$$X = FH, OH_2, NH_3, N_2, OC, CO, CH_2\ (^1A_1)$$
$$Y_2 = H_2$$
(type III complexes)

Hence, type III complexes may be considered as a combination of type I and type II complexes. It will be seen that the structures of CH_4X^{2+} can best be understood when they are considered as the result of competition between X and Y to donate electrons to CH_2^{2+}.

The strength of the donor–acceptor interaction is determined mainly by the frontier orbitals of the respective donor and acceptor molecules. Further insight into the electronic structure is achieved by using the one-electron density analysis. While most readers can be assumed to be familiar with the concepts of donor–acceptor interaction and frontier orbitals,[21] this may not hold for the density analysis. The theoretical background of this technique has been described in detail somewhere else.[22-24] Here we focus on the

(6) Lammertsma, K.; Barzaghi, M.; Olah, G. A.; Pople, J. A.; Kos, A. J.; Schleyer, P. v. R. *J. Am. Chem. Soc.* **1983**, *105*, 5252.

(7) (a) Olah, G. A.; Simonetta, M. *J. Am. Chem. Soc.* **1982**, *104*, 330. (b) Schleyer, P. v. R.; Kos, A. J.; Pople, J. A.; Balaban, A. T. *J. Am. Chem. Soc.* **1982**, *104*, 3771. (c) Koch, W.; Frenking, G.; Schwarz, H.; Maquin, F.; Stahl, D. *Int. J. Mass Spectrom. Ion Proc.* **1985**, *63*, 59. (d) Lammertsma, K. *J. Am. Chem. Soc.* **1984**, *106*, 4619. (e) Bouma, W. J.; Radom, L. *J. Am. Chem. Soc.* **1983**, *105*, 5484.

(8) (a) Cooper, D. L.; Wilson, S. *Mol. Phys.* **1981**, *44*, 161. (b) Frenking, G.; Koch, W. *J. Chem. Soc., Chem. Commun.*, in press. Koch, W.; Frenking, G. *J. Chem. Phys.*, submitted.

(9) Lammertsma, K.; Schleyer, P. v. R. *J. Am. Chem. Soc.* **1983**, *105*, 1049.

(10) (a) Krogh-Jespersen, K.; Cremer, D.; Dill, J. D.; Pople, J. A.; Schleyer, P. v. R. *J. Am. Chem. Soc.* **1981**, *103*, 2589. (b) Chandrasekhar, J.; Schleyer, P. v. R.; Krogh-Jespersen, K. *J. Comput. Chem.* **1981**, *2*, 356.

(11) (a) Hogeveen, H.; Kwant, P. W. *J. Am. Chem. Soc.* **1974**, *96*, 2208. (b) Hogeveen, H.; Kwant, P. W. *Acc. Chem. Res.* **1975**, *8*, 413.

(12) (a) Lammertsma, K.; Olah, G. A.; Barzaghi, M.; Simonetta, M. *J. Am. Chem. Soc.* **1982**, *104*, 6851. (b) Lammertsma, K.; Barzaghi, M.; Olah, G. A.; Pople, J. A.; Schleyer, P. v. R.; Simonetta, M. *J. Am. Chem. Soc.* **1983**, *105*, 5258.

(13) (a) Schwarz, H. *Nachr. Chem. Tech. Lab.* **1983**, *31*, 451. (b) Schwarz, H. *Mass Spectrom.* **1984**, *32*, 3.

(14) Radom, L.; Bouma, W. J.; Nobes, R. H.; Yates, B. F. *Pure Appl. Chem.* **1984**, *56*, 1831.

(15) (a) Lathan, W. A.; Curtiss, L. A.; Hehre, W. J.; Lisle, J. B.; Pople, J. A. *Prog. Phys. Org. Chem.* **1974**, *11*, 175. (b) Terlouw, J. K.; Heerma, W.; Dijkstra, G.; Holmes, J. L.; Burgers, P. C. *Int. J. Mass Spectrom. Ion Phys.* **1983**, *47*, 147. (c) Holmes, J. L.; Lossing, F. P.; Terlouw, J. K.; Burgers, P. C. *J. Chem.* **1983**, *61*, 2305. (d) Bouma, W. J.; Yates, B. F.; Radom, *Chem. Phys. Lett.* **1982**, *92*, 620. (e) Halim, H.; Ciommer, B.; Schwarz, H. *Angew. Chem., Int. Ed. Engl.* **1982**, *21*, 528.

(16) (a) Frisch, M. J.; Raghavachari, K.; Pople, J. A.; Bouma, W. J.; Radom, L. *Chem. Phys.* **1983**, *75*, 323. (b) Holmes, J. L.; Lossing, F. P.; Terlouw, J. K.; Burgers, P. C. *J. Am. Chem. Soc.* **1982**, *104*, 2931. (c) Bouma, W. J.; Nobes, R. H.; Radom, L. *J. Am. Chem. Soc.* **1982**, *104*, 2929. (d) Bouma, W. J.; MacLeod, J. K.; Radom, L. *J. Am. Chem. Soc.* **1982**, *104*, 2930.

(17) (a) Bouma, W. J.; Dawes, J. M.; Radom, L. *Org. Mass Spectrom.* **1983**, *18*, 12. (b) Yates, B. F.; Nobes, R. H.; Radom, L. *Chem.* Phys. *Lett.* **1985**, *116*, 474.

(18) Frenking, G.; Koch, W. *J. Mol. Struct. (THEOCHEM)* **1984**, *110*, 49.

(19) Maquin, F.; Stahl, D.; Sawaryn, A.; Schleyer, P. v. R.; Koch, W.; Frenking, G.; Schwarz, H. *J. Chem. Soc. Chem. Commun.* **1984**, 504.

(20) The names ylide ion and ylide dication have been proposed (ref 14) for the singly and doubly charged structures such as $H_2C{-}OH_2^{n+}$ ($n = 1, 2$) since they correspond formally to ionized ylides. While the term "complex" may not seem to be appropriate for structures such as **11** or **20**, we prefer the name donor–acceptor complexes in the context of our investigation in order to emphasize our structural approach, and also because it is more general and covers species which are not ionized ylides.

(21) (a) Fleming, I. *Frontier Orbitals and Organic Chemical Reactions*; Wiley: New York, 1976. (b) Fukui, K. *Acc. Chem. Res.* **1971**, *4*, 57.

(22) Bader, R. F. W.; Nguyen-Dang, T. T.; Tal, Y. *Rep. Prog. Phys.* **1981**, *44*, 893.

application of this method, and we will present in the next section only a short outline of the basic ideas in such a way that the nontheoretician can also use the information which is given here. Previous attempts to combine MO and electron density analysis have proven to be very successful,[22-26] producing more reliable and comprehensive information of the electronic structure of molecules compared to familiar concepts such as the Mulliken population analysis.[27]

II. Quantum Chemical Methods

All MO calculations in this study have been performed with the CRAY version of GAUSSIAN 82.[28] Geometry optimizations were carried out with a 6-31G* basis set. Additional single-point calculations include electron correlation incorporated at the third-order Møller–Plesset level of perturbation theory (frozen core).[29] Hence, total energies have been obtained at the MP3/6-31G*//6-31G* level of theory.

The one-electron density distribution $\rho(r)$ is analyzed with the aid of its gradient vector field $\nabla\rho(r)$ and the Laplacian $\nabla^2\rho(r)$.[30] Previous investigations have shown that $\rho(r)$ exhibits local maxima only at the positions of the nuclei. Bonded atoms are linked by a path of maximum electron density, called bond path.[23] The bond path can be considered as an image of the bond. A model has been developed to distinguish and to characterize covalent, ionic, hydrogen, and van der Waals bonds.[24] The network of bond paths (bonds) linking a collection of atoms defines the molecular structure.[31]

Covalent bonds can be described by the properties of $\rho(r)$ at the bond critical point r_b. The latter corresponds to the minimum of ρ along the bond path and, hence, to a saddle point of ρ in three dimensions. From the value of $\rho_b \equiv \rho(r_b)$ a bond order n can be defined:[22,24]

$$n = \exp[A(\rho_b - B)]$$

with constants A and B depending on the nature of the atoms bonded together.[32]

Examination of the various quantities obtained in the one-electron analysis also showed that the matrix of second derivatives of $\rho(r_b)$ (Hessian matrix) provides valuable information in regard to the electronic structure. The eigenvalues of the Hessian matrix yield the Laplacian of $\rho(r_b)$, $\nabla^2\rho(r_b)$. A negative (positive) value of $\nabla^2\rho(r)$ is indicative of local charge concentration (depletion) at r.[25,26,30a] The distribution $\nabla^2\rho(r)$ has been found to reflect the shell structure of atoms. In molecules, concentration lumps can be associated to electron bonds and electron lone pairs on the basis of simple models.[30b]

In order to characterize the energetic aspects of a bond, the energy density $H(r)$ has been defined.[24] A value of $H(r_b) \equiv H_b$ smaller (larger) than 0 indicates that electron density at the bond critical point r_b is (de)stabilizing. It has been suggested to consider the existence of a bond path as a necessary and $H_b < 0$ as a sufficient condition for the existence of a covalent bond.[24]

III. Results and Discussion

The calculated total energies of the neutral donor molecules X **1–9**, the acceptor dications CH_2^{2+} **10** and CH_4^{2+} **11**, and the donor–acceptor complexes CH_2X^{2+} **20–28** and CH_4X^{2+} **28–37** are listed in Table I. Structure **28** may formally be considered as belonging to both classes of donor–acceptor complexes, while CH_4^{2+} **11** represents formally the complex of $CH_2^{2+} + H_2$. The optimized geometries are shown in Chart I. While some of the total energies have previously been reported,[5b,6,7d,e,12,33] only the complete geometries of the donor–acceptor complexes **11**,[5b] **20**,[6] **22**,[7e] and **36**[12b] are given in the literature. In order to discuss the results of donor–acceptor interaction, they are included in Chart I, together with the geometries of **1–11**, taken from published data.[33]

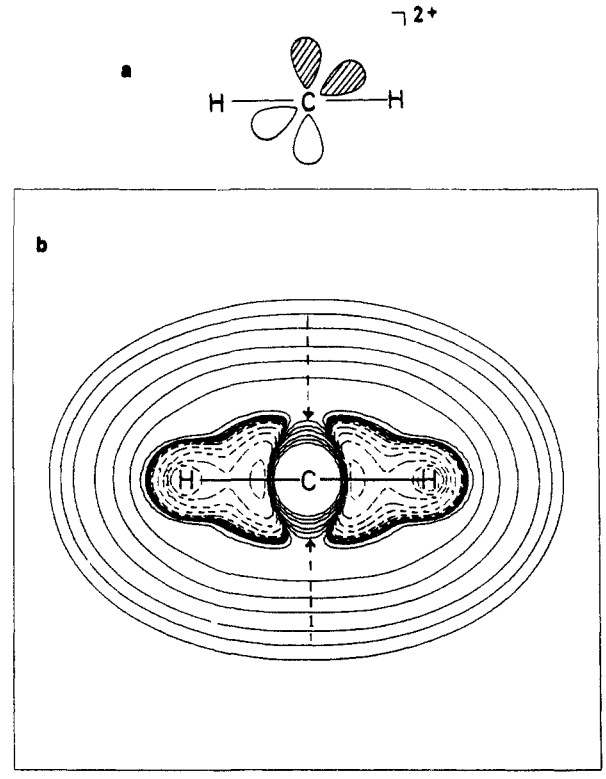

Figure 1. (a) Schematic representation of the pπ MOs of CH_2^{2+}. (b) Contour line diagram of $\nabla^2\rho(r)$ of CH_2^{2+} calculated at the HF/6-31G* level of theory. Dashed lines indicate a value of $\nabla^2\rho(r) < 0$ (charge concentration) and solid lines a value of $\nabla^2\rho(r) > 0$ (charge depletion). The Laplacian of $\rho(r)$ is not shown for the inner-shell area of C. Heavy solid lines denote bond paths (paths of maximum electron density between atomic nuclei). The heavy dashed arrows point to the concentration hole in the valence sphere of the C atom.

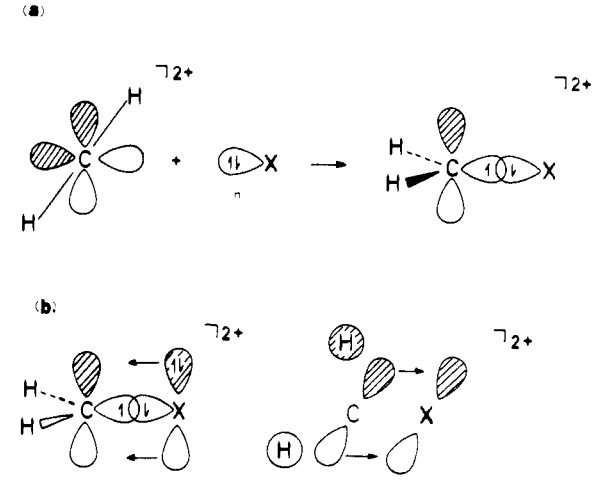

Figure 2. Schematic presentation of the interaction of CH_2^{2+} with (a) a σ-donor X and (b) a σ/π-donor (π-acceptor) X.

(1) The Parent Dication CH_2^{2+} (10). Since we consider all dications **11–37** as donor–acceptor complexes of **10** and one or two neutral closed-shell molecules, it is advisable to discuss MOs and density features of CH_2^{2+} first. **10** possesses a linear geometry, which can be considered as the result of maximum overlap between sp-hybridized C orbitals and the 1s (H) orbitals. In addition,

(23) (a) Bader, R. F. W.; Slee, T. S.; Cremer, D.; Kraka, E. *J. Am. Chem. Soc.* **1983**, *105*, 5061. (b) Cremer, D.; Kraka, E.; Slee, T. S.; Bader, R. F. W.; Lau, C. D. H.; Nguyen-Dang, T. T.; MacDougall, P. J. *J. Am. Chem. Soc.* **1983**, *105*, 5069.

(24) Cremer, D.; Kraka, E. *Croat. Chem. Acta* **1985**, *57*, 1265 (1985).

(25) Cremer, D.; Kraka, E. *Angew. Chem.* **1984**, *96*, 612; *Angew. Chem. Int. Ed. Engl.* **1984**, *23*, 627.

(26) Cremer, D.; Kraka, E. *J. Am. Chem. Soc.* **1985**, *107*, 3800, 3811.

(27) Mulliken, R. S. *J. Chem. Phys.* **1955**, *23*, 1833.

(28) Binkley, J. S.; Frisch, M. J.; DeFrees, D. J.; Raghavachari, K.; Whiteside, R. A.; Schlegel, H. B.; Fluder, E. M.; Pople, J. A., Carnegie-Mellon University, Pittsburgh.

(29) (a) Møller, C.; Plesset, M. S. *Phys. Rev.* **1934**, *46*, 618. (b) Binkley, J. S.; Pople, J. A. *Int. J. Quantum Chem.* **1975**, *9S*, 229.

(30) (a) Bader, R. F. W.; MacDougall, P. J.; Lau, C. D. H. *J. Am. Chem. Soc.* **1984**, *106*, 1594. (b) Bader, R. F. W.; Essen, H. *J. Chem. Phys.* **1984**, *80*, 1943.

(31) Bader, R. F. W.; Tal, Y.; Anderson, S. G.; Nguyen-Dang, T. T. *Isr. J. Chem.* **1980**, *19*, 8.

(32) The constants A and B depend also on the basis set used. In the case of HF/6-31G* calculations A and B adopt the following values: 0.94, 1.52 e/Å^3 (CC); 0.78, 1.87 e/Å^3 (CN); 0.65, 1.77 e/Å^3 (CO).[24]

(33) Whiteside, R. A.; Frisch, M. J.; Pople, J. A. *The Carnegie-Mellon Quantum Chemistry Archive*, 3rd ed.; Carnegie-Mellon University: Pittsburgh, 1983.

Table I. Calculated Total Energies (hartrees) at the HF/, MP2/, and MP3/6-31G* Level, Using 6-31G* Optimized Geometries. (The Energies for Structures **1–9** have been Taken from Reference 33. All Other Data Are Our Results Unless Otherwise Noted)

	donor X, acceptor molecules						CH_2^{2+} (**10**) + X				CH_4^{2+} (**11**) + X			
no.	molec.	symm	HF	MP2	MP3	no.	symm	HF	MP2	MP3	no.	symm	HF	MP2	MP3
1	CH_2 ($^1A_1$)	C_{2v}	−38.8724	−38.9699	−38.9877	**20**	D_{2d}	−77.0867[b]	−77.2719	−77.2986	**28**	C_s	−78.2622	−78.4924	−78.5205
2	NH_3	C_{3v}	−56.1844	−56.3537	−56.3654	**21**	C_s	−94.3609[c]	−94.6156	−94.6388	**29**	C_s	−95.5325[c]	−95.8325	−95.8576
3	OH_2	C_{2v}	−76.0108	−76.1959	−76.2019	**22**	C_{2v}	−114.1293[d]	−114.4052	−114.4197	**30**	C_s	−115.2807[c]	−115.5918	−115.6110
4	FH	$C_{\infty v}$	−100.0029	−100.1816	−100.1834	**23**	C_{2v}	−137.9706	−138.2349	−138.2447	**31**	C_s	−139.1733	−139.4796	−139.4937
5	CO	$C_{\infty v}$	−112.7379	−113.0180	−113.0173	**24**	C_{2v}	−150.7543[e]	−151.1343	−151.1375	**32**	C_{4v}	−151.9676	−152.3961	−152.4008
	OC	$C_{\infty v}$	−112.7379	−113.0180	−113.0173	**25**	C_{2v}	−150.7209	−151.0677	−151.0864	**33**	C_s	−151.9012	−152.2939	−152.3125
6	N_2	$D_{\infty h}$	−108.9440	−109.2481	−109.2453	**26**	C_{2v}	−146.9241[c]	−147.3139	−147.3228	**34**	C_s	−148.1224[e]	−148.5595	−148.5688
7	F_2	$D_{\infty h}$	−198.6778	−199.0305	−199.0303	**27**	C_{2v}	−236.7231	−237.1931	−237.1852	**35**	C_s	−237.7933	−238.2705	−238.2824
8	H_2	$D_{\infty h}$	−1.1268	−1.1441	−1.1492	**11**	D_{4h}	−39.0469[a]	−39.1506	−39.1679	**36**	C_{2v}	−40.2768[d]	−40.4271	−40.4451
9	CH_4	T_d	−40.1952	−40.3325	−40.3485	**28**	C_s	−78.2622	−78.4924	−78.5205	**37**	C_2	−79.4171	−79.7006	−79.7299
10	CH_2^{2+}	$D_{\infty h}$	−37.8004[a]	−37.8613	−37.8753										
11	CH_4^{2+}	D_{4h}	−39.0469[a]	−39.1506	−39.1679										

[a] Reference 5b. [b] Reference 6. [c] Reference 7d. [d] Reference 12b.

Table II. Calculated Reaction Energies (kcal/mol) for Reactions 1, 2, and 3 at the MP3/6-31G*//6-31G* Level

X	reaction 1	reaction 2	reaction 3
CH_2 ($^1A_1$)	−273.3	−229.0	−45.6
NH_3	−249.8	−203.5	−43.7
OH_2	−214.9	−151.4	−26.4
FH	−116.7	−89.4	−62.6
CO	−153.7	−135.3	−71.6
OC	−121.6	−79.9	−48.3
N_2	−126.9	−97.6	−60.7
F_2	−175.4	−52.8	+32.6
H_2	−90.0	−80.3	−80.3
CH_4	−186.2	−134.0	−37.8

Table III. Theoretically (MP3/6-31G*//6-31G*) and Experimentally Derived Proton Affinities (kcal/mol) of the Donor Molecules X

X	calcd	exptl
CH_2 ($^1A_1$)	−221.9	
NH_3	−217.9	−207[a]
OH_2	−175.1	−164[a]
FH	−124.6	−112[b]
CO	−145.4	−143,[a] −139[b]
OC	−107.6	
N_2	−120.3	−116,[a] −114[b]
F_2	−89.2	
H_2	−95.9	−101[b]
CH_4	−125.1	−126,[a] −128[b]

[a] Reference 40. [b] Reference 41.

destabilizing electrostatic interactions between positively charged H atoms favor a linear geometry. Due to charge repulsion, the C–H bonds are longer in sp-hybridized CH_2^{2+} compared to sp_2-hybridized CH_2 ($^1A_1$).

There are two vacant degenerate pπ orbitals at C (Figure 1a). This is reflected in the Laplace field of $\rho(r)$ (Figure 1b) by holes of the charge concentration in the valence sphere of C, which form a torus surrounding the carbon atom perpendicular to the molecular axis.

(2) Type I Dications CH_2X^{2+}. If electronic charge is donated from a lone-pair orbital of a neutral molecule X to the vacant pπ orbitals of **10**, a donor–acceptor complex of type I is formed. Examples are structures **20–26**. Rehybridization at the C atom from sp to sp^2 increases the orbital interactions between donor and acceptor (Figure 2a). The donor X may also possess filled pπ orbitals, which can donate electrons to the second pπ(C) orbital of CH_2^{2+}. In addition, some donors X have empty or low-lying π^* MOs allowing back-donation from the pseudo-π C–H orbitals of CH_2^{2+} (hyperconjugation), thus increasing interactions between **10** and X (Figure 2b). The actual strength of the CX bond will depend on the σ- (and π-) donor and π-acceptor ability of X.

The strength of the donor–acceptor interaction in **20–26** can be determined by calculating the reaction energies dE_R of reaction 1 for type I dications:

$$CH_2X^{2+} + H_2 \rightarrow CH_2X(H_2)^{2+} + \Delta E_R \qquad (1)$$

The results shown in Table II establish the following order of donor strength for X in type I dications:

$$CH_2 > NH_3 > OH_2 > CO > N_2 > OC > FH$$

This may be compared with the theoretically and experimentally determined proton affinities listed in Table III which show the sequence

$$NH_3 > OH_2 > CO > N_2 \sim FH \qquad \text{(exptl)}$$

$$CH_2 > NH_3 > OH_2 > CO > FH > N_2 > OC \qquad \text{(calcd)}$$

The comparison shows that (i) the stabilization sequence for the donor molecules X obtained for reaction 1 is very similar to what is found for the proton affinities of X; (ii) the computed values for ΔE_R of reaction 1 (117–273 kcal/mol) are always larger

Chart I. Optimized Geometries (6-31G*) of Structures **1**–**37**. Bond Lengths Are Given in Å and Angles in Deg

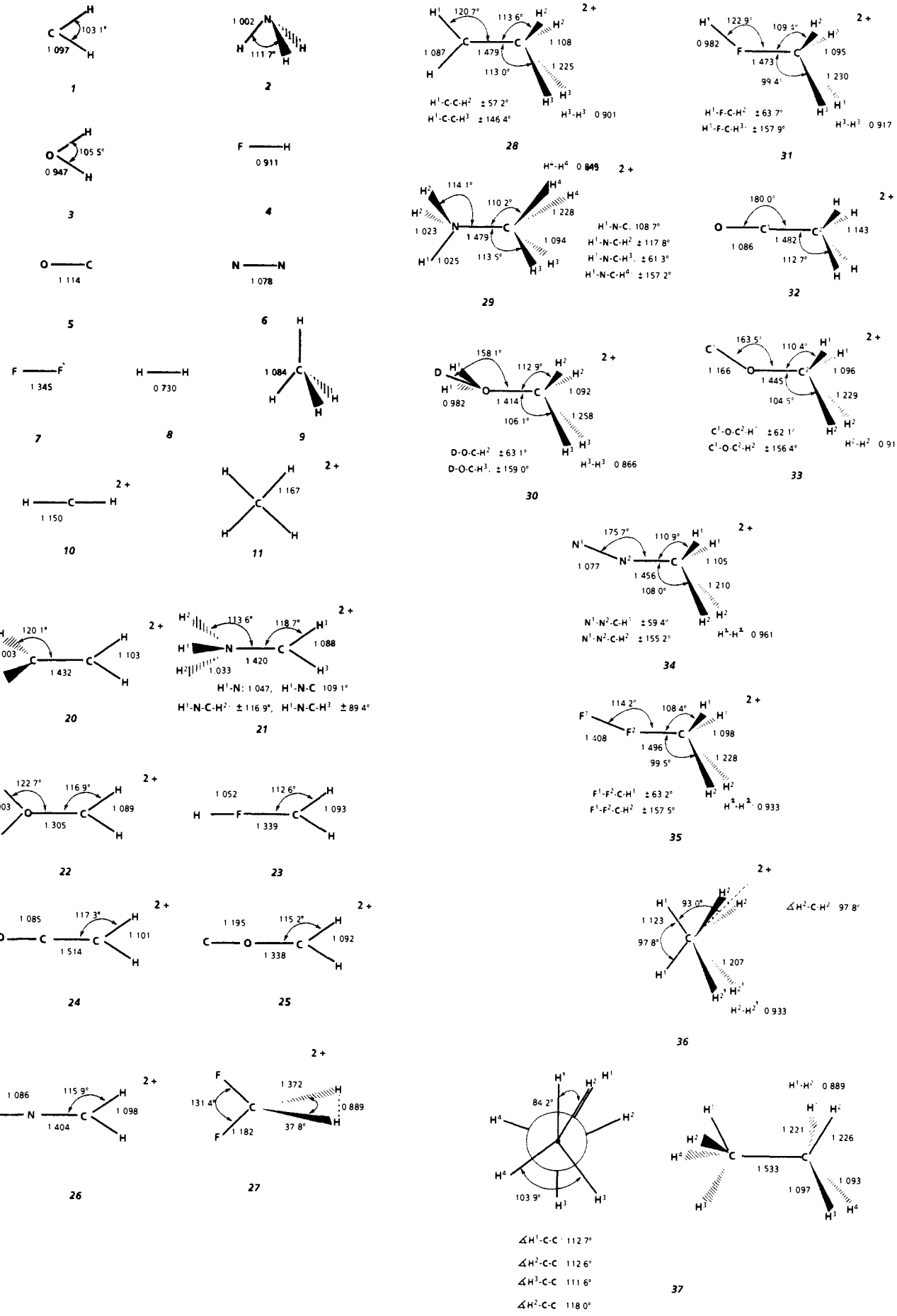

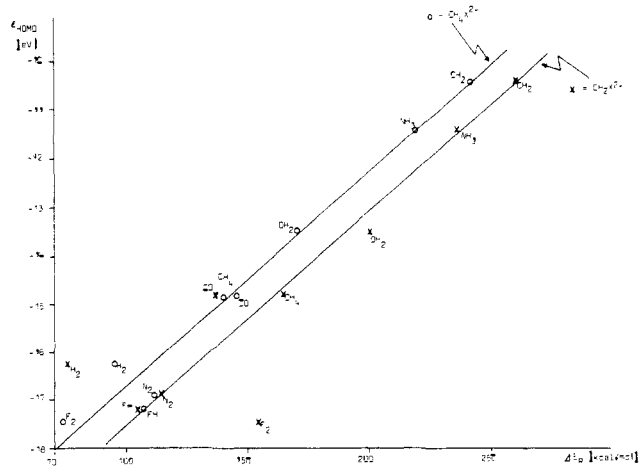

Figure 3. Correlation of the eigenvalues of the frontier orbitals ϵ_{HOMO} of the donor molecules X (eV) with calculated reaction energies of reaction 1 (×) and 2 (○) (kcal/mol, Table II).

Table IV. Properties of CX Bonds of Dications CH_2X^{2+} as Reflected by the Properties of Electron and Energy Density[a]

X	ρ_b (e/Å^3)	$\nabla^2\rho_b$ (e/Å^5)	H_b (hartree/Å^3)	n
FH[a]	1.426	21.265	−1.620	<1
OC	1.727	14.655	−2.314	0.97
CO	1.760	−20.303	−1.711	1.25
N_2	1.797	−6.126	−2.763	0.94
OH_2[a]	2.040	11.939	−2.993	1.19
NH_3[a]	2.104	−31.650	−3.086	1.20
CH_2 ($^1A_1$)	2.170	−25.953	−2.225	1.84

[a] Values of ρ_b, $\nabla^2\rho_b$, and H_b can be compared with the following reference values: 1.606, 12.914, −2.125 (CH_3F); 1.775, −3.493, −2.665 (CH_3OH); 1.866, −22.762, −2.571 (CH_3NH_2).[24]

but have the same order of magnitude as compared to the calculated proton affinities (80–229 kcal/mol) (Table III). The rather high ΔE_R values point to strong C–X bonding in these "complexes".[20]

What determines the donor strength of X in CH_2X^{2+}? In Figure 3, the eigenvalues of the highest occupied molecular orbital (HOMO) of X are plotted against the reaction energies ΔE_R of reaction 1. The correlation is obvious. Molecules X with a higher lying HOMO are better donors and show larger stabilization energies ΔE_R compared to species with a lower lying HOMO. This is exactly what frontier orbital theory predicts.[43]

A comparison of the geometries of **20–26** with those of the separated donor and acceptor molecules (Chart I) reveals structural features which can be explained by the order of donor–acceptor interaction. Donation of electronic charge from X to CH_2^{2+} leads to bending of HCH and shortening of the C–H bonds in CH_2^{2+}.[34] Although steric interaction and hyperconjugation are additional factors determining the geometry, the magnitude of these changes follows quite closely the sequence of donor ability established above. At the same time, the bonds in the donor X become longer due to electron depletion. A notable exception is CO, which is discussed in detail below. While the interaction of the frontier orbitals[21] accounts for most of the features found for the type I dications **20–26**, the electron density analysis will show a more detailed picture of their electronic structure.

Relevant electron density properties determined at the bond critical point r_b of the CX bond of type I complexes are summarized in Table IV. In agreement with the calculated stabilization energies dE_R for reaction 1, they reveal that all CX bonds are relatively strong with bond orders n close to 1 or even larger than 1 (Table IV). For **20**, nearly a double bond is found due to strong hyperconjugation, which supports earlier conclusions.[6,35] The bond orders n confirm the order of CX bond strengths established by reaction 1.

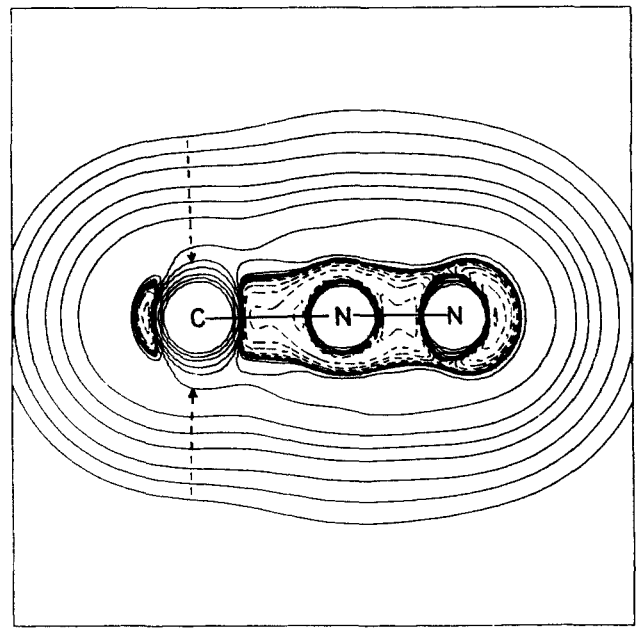

Figure 4. Contour line diagram of $\nabla^2\rho(r)$ of $CH_2N_2^{2+}$ taken in the plane perpendicular to the molecular plane and containing the three heavy atoms. For further information see the caption for Figure 1b.

The strength of the CX bonds is also reflected by the values of ρ_b, $\nabla^2\rho_b$, and H_b when they are compared with the values obtained for appropriate reference bonds (Table IV). The C–F bond in $H_2C{-}FH^{2+}$ is found to be weaker compared to CH_3F, while the C–O and C–N bonds in the dications are stronger in comparison to the reference compounds CH_3OH and CH_3NH_2. According to the criterium suggested by Cremer and Kraka ($H_b < 0$),[24] all bonds are covalent.

The bending and bond shortening of CH_2^{2+} in **20–26** can be analyzed with the aid of the properties of $\rho(r)$ obtained for the free closed-shell molecules X (Table V). In all cases with the exception of X = CO, the bonds in X are weakened. Weakening depends on the polarity of the bonds which becomes obvious when comparing ρ-properties for AH bonds in the series X = AH_n = FH, OH_2, NH_3, CH_2. For X = FH one finds the largest decrease in ρ_b(AH) upon complexation, while for X = CH_2 the smallest change is found. At the same time the AH bond polarity as measured by ρ_b is increased. Electron density is pulled from the H atoms toward A to compensate for the loss of electrons donated to CH_2^{2+}.

Similar observations can be made for X = AB when the electronegativity of the atom A bonded to CH_2^{2+} is greater or comparable to that of B (X = OC and N_2). If the electronegativity of B is larger than that of A (X = CO), the direction of charge migration caused by complexation reduces the bond polarity and causes an increase rather than a decrease of the AB bond strength which can be illustrated by writing appropriate mesomeric formulas:

$$H_2C^{2+}\,\overset{-}{A}{-}\overset{-}{B} \leftrightarrow H_2\overset{+}{C}{-}\overset{+}{A}{-}\overset{-}{B} \leftrightarrow H_2\overset{+}{C}{-}A{=}\overset{+}{B}$$

This explains why the C–O bond distance is smaller in the donor–acceptor complex **24** compared with that in isolated CO (Chart I).

In Figure 4 the distribution $\nabla^2\rho(r)$ of $CH_2N_2^{2+}$ (**26**) is shown in the form of a contour line diagram in a plane containing the three heavy atoms and being perpendicular to the molecular plane.

(34) Bending of the CH_2 unit is accompanied with rehydridization at C from sp toward sp_2, and hence longer C–H bonds might be expected. However, electronic charge from the donor leads to a decrease in coulomb repulsion, and the net effect is always a shorter bond. This is corroborated by the observation that the decrease in C–H bond length runs parallel to the donor strength.

(35) Frenking, G.; Koch, W.; Schwarz, H. *J. Comput. Chem.*, in press.

Table V. Comparison of Free and Complexed X in CH_2X^{2+} on the Basis of $\rho(r)$ and $H(r)$

X	form	bond	ρ_b (e/Å^3)	$\nabla^2\rho_b$ (e/Å^5)	H_b (hartree/Å^3)	Δ_b[a] (%)
FH	free	F-H	2.421	-68.979	-5.332	-67.9
	complex		1.003	-37.077	-2.698	-76.2
OC	free	O-C	3.372	41.543	-5.527	-34.0
	complex		2.478	24.705	-3.558	-35.4
CO	free	C-O	3.372	41.543	-5.527	34.0
	complex		3.589	56.782	-6.106	32.9
NN	free	N-N	4.801	-66.499	-8.776	0
	complex		4.492	-60.657	-8.243	-8.1
OH_2	free	O-H	2.476	-50.159	-3.959	-61.0
	complex		1.837	-48.621	-3.557	-69.4
NH_3	free	N-H	2.312	-41.739	-3.272	-49.3
	complex[b]		2.018	-38.210	-2.832	-59.4
CH_2 ($^1A_1$)	free	C-H	1.908	-25.285	-1.980	-28.3
	complex		1.840	-31.100	-2.242	-46.3

[a] Δ_b denotes the deviation of the bond critical point r_b from the midpoint of the bond considered.[24] A negative (positive) Δ_b corresponds to a shift of r_b toward the second (first) atom of the bond. [b] Averaged values.

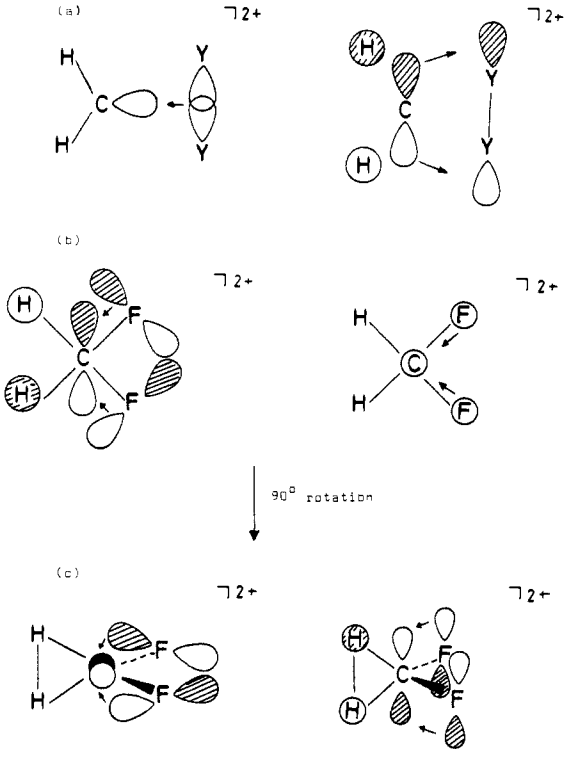

Figure 5. Schematic representation of (a) interaction of CH_2^{2+} with Y_2; orbital interaction in (b) planar and (c) tetrahedral $CF_2H_2^{2+}$.

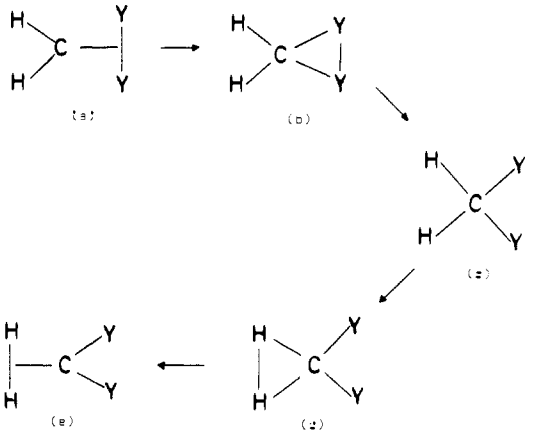

Figure 6. Structure diagrams of $CH_2(Y_2)^{2+}$.

Table VI. Properties of CH and CX Bonds in Doubly Charged and Neutral Molecules, Respectively.

molecule	bond	ρ_b (e/Å^3)	$\nabla^2\rho_b$ (e/Å^5)	H_b (hartree/Å^3)
CH_4^{2+}	C-H	1.386	-21.648	-1.549
CH_4	C-H	1.869	-23.581	-1.914
$CF_2H_2^{2+}$	C-H	1.072	-6.032	-0.483
	C-F	2.774	20.509	-4.392
	H-H	1.064	-5.177	-0.395
CF_2H_2	C-H	2.080	-30.443	-2.296
	C-F	1.745	10.859	-2.407

The $\nabla^2\rho(r)$ diagram displays the charge concentration between C and N but also the holes in the charge concentration in the valence sphere of carbon above and below the molecular plane. These holes are found for all type I dications. They reveal that CH_2X^{2+} is capable of interacting with another donor.

(3) Type II Dications $CH_2Y_2^{2+}$. From a structural point of view, type II dications are more interesting than type **I** dications. Type II dications are formed if electron density is transfered from bonding σ-MOs rather than lone-pair orbitals of the donor molecules to CH_2^{2+} (CY_2^{2+}) (Figure 5a). Structures **11** and **27** are examples investigated here. In addition, there can be back-donation from the pseudo-π orbital of the CH_2^{2+} (CY_2)$^{2+}$ group to $\sigma^*(Y_2)$ ($\sigma^*(H_2)$) (Figure 5a). Depending on the strength of the two types of interactions, the structural situations shown in Figure 6 can develop: (a) The $\sigma(Y_2)$ MO is low in energy. Only a small amount of charge is donated. There is no back-donation. A loose complex with a T-structure (Figure 6, a) is formed. (b) π-back-donation from CH_2 is stronger than σ-donation leading to bond paths between Y and C. A three-membered ring structure is formed (Figure 6, b). (c) σ-donation from the $\sigma(Y_2)$ MO is fully developed, as is π-back-donation into the $\sigma^*(Y_2)$ MO. An open structure developes, and the Y-Y σ-bond is broken (Figure 6, c). The latter situation applies to CH_4^{2+} **11** where Y_2 and H_2 are identical which leads to a square-planar structure. (d) In the way σ-donation and π-back-donation between CH_2^{2+} and Y_2 increase, the CY bonds become stronger at the expense of the CH bonds. Thus, $CH_2Y_2^{2+}$ eventually changes to a donor-acceptor complex between CY_2^{2+} and H_2, again with the possibility of adopting a ring or a T-structure (Figures 6, d and e).

In the case of $Y_2 = F_2$ (**27**), there is competition between electron donation from H_2 and F_2. The H-H bond is much stronger compared to the F-F bond, making F_2 a better σ-donor. In addition, the F atoms can donate π-electron to the empty pπ(C) orbital (Figure 5b) thus enhancing the strength of the CF bonds. At the same time, the CH bonds are weakened by electron donation from the n_- ($n_{F1}-n_{F2}$) in-plane combination of lone-pair orbitals into the CH_2 pseudo-π^* MO (Figure 5b). However, the molecule can stabilize by changing from a planar to a perpendicular arrangement of the CF_2 and H_2 entities (Figure 5c). Although there are again two kinds of orbital interaction, one which strengthens the CF bonds and one which weakens the CH bonds, the overall effect is now more stabilizing since orbital overlap has been increased for the first kind of interaction and decreased for the second one (Figure 5c). As a result $CF_2H_2^{2+}$ **27** adopts the three-membered ring structure (Figure 6, d) as is

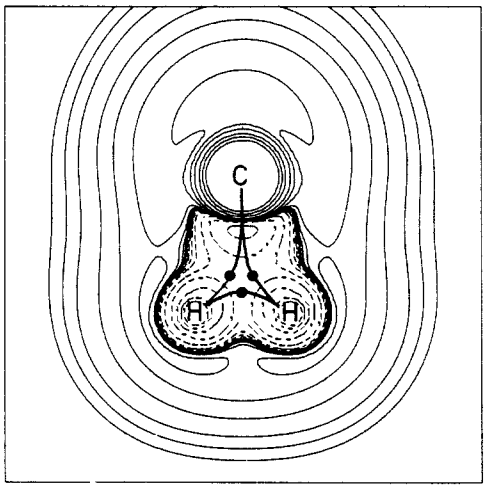

Figure 7. Contour line diagram of $\nabla^2\rho(r)$ of $CF_2H_2^{2+}$ taken in the plane which contains C and the two H atoms. Bond critical points are denoted by dots. For further information see the caption for Figure 1b.

verified by the data given in Table VI and the $\nabla^2\rho$ plot for **27** depicted in Figure 7. The latter reveals that electron density is totally delocalized in the HHC plane between the three nuclei, which are connected by bond paths (solid lines in Figure 7).

The discussion presented above indicates that the electronic structure of $CH_2F_2^{2+}$ **27** cannot simply be considered as frontier orbital interaction between CH_2^{2+} and F_2. Thus, the calculated stabilization energy for X = F_2 in reaction 1 (-175.4 kcal/mol, Table II) is much larger as it might have been predicted from the computed proton affinity of F_2 (89.2 kcal/mol, Table III). For X = H_2, however, the calculated values for ΔE_R of (1) and proton affinity agree with the sequence of donor ability predicted for various donors X (Tables II and III).

The optimized structure **27** for $CH_2F_2^{2+}$ corresponds to donor-acceptor interaction between CF_2^{2+} and H_2, rather than CH_2^{2+} and F_2. We calculated the energy of hydrogenation of CF_2^{2+} leading to $CH_2F_2^{2+}$ **27**. At the MP3/6-31G*//6-31G* level, the reaction energy is -59.4 kcal/mol.[44] This is much less compared to the hydrogenation reaction of CH_2^{2+} (-90.0 kcal/mol, Table II). The eigenvalue ϵ_{LUMO} of CF_2^{2+} is substantially lower (-16.07 eV, 6-31G*/6-31G*)[44] compared with CH_2^{2+} (-19.25 eV, 6-31G*/6-31G*). Thus, the lower hydrogenation energy of CF_2^{2+} is explained by frontier orbital interaction.

(4) Type III Dications $CH_2X(Y_2)^{2+}$. Due to the fact that there are still large charge-concentration holes in the valence sphere of carbon (corresponding to vacant pπ orbitals) in CH_2X^{2+} dications (Figure 4), a second donor either of type X (with a lone-pair orbital) or type Y_2 can be coordinated at C. In this work we consider only the latter case with Y_2 = H_2, i.e., structures **28-36**, which may therefore be considered as hydrogenated forms of **20-27**. **37** is a special case which arises from doubly hydrogenated **20** (or singly hydrogenated **28**). This has already been recognized by Lammertsma et al.[12b]

In Figure 8 orbital interactions between the two donor molecules X and H_2 and the acceptor CH_2^{2+} are shown. Donation from an n-orbital will always be stronger than that from the $\sigma(H_2)$ MO (Figure 8a). Besides donation from the (σ-type) lone-pair orbital, some of the donors X can donate electronic charge from filled π-orbitals into the empty pπ(C) orbital (Figure 8a) and pseudo-π MO of CH_2^{2+} (Figure 8b). However, there is now competition for electron donation into the empty pπ(C) orbital between $\sigma(H_2)$ and $\pi(X)$ orbitals (Figure 8). Furthermore, back-donation of the partially filled pπ(C) orbital into the π^* MO is possible for some donors X (Figure 8c). Hence, H_2 donation will depend on the extend and type of X donation, as will the degree of back-donation from the pseudo-π MO of CH_2 to $\sigma^*(H_2)$ (Figure 8b). As in the case of $CH_2(Y_2)^{2+}$ dications (Figure 6), one can expect open, ring, and T structures for $CH_2X(H_2)^{2+}$ dications. The actual structure and the specific geometry of type III dications will depend on the relative donor ability of X.

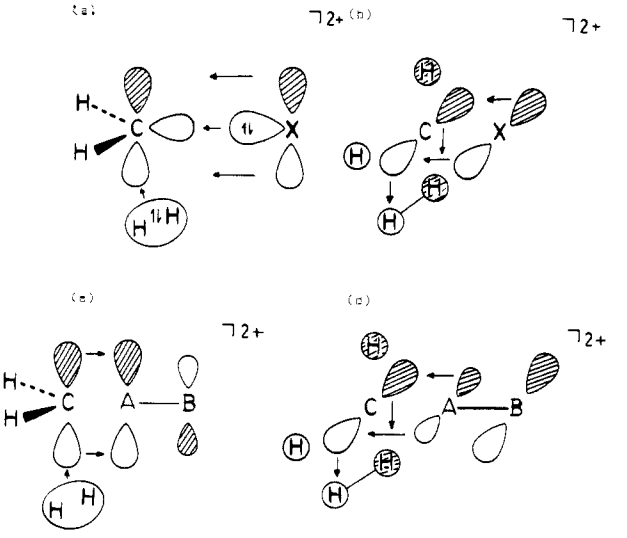

Figure 8. Schematic representation of interaction of donors X and H_2 (a) with $\sigma\pi$ and pπ orbitals of CH_2^{2+} and (b) with the pseudo-π orbital of CH_2^{2+}. Orbital interactions for donors X = AB involving (a) the pπ orbital of CH_2^{2+} and (b) the pseudo-π MO of CH_2^{2+}.

Table VII. Structure of the $C(H_2)$ Unit of $CH_2X(H_2)^{2+}$ Dications in Dependence on the Structure of X

X	R(H-H) (Å)	ρ_b(C-H) (e/Å^3)	structure characterization of X	
CO	1.492	1.478	open	σ/π-donor, π-acceptor
NN	0.961	1.364	open	σ/π-donor, π-acceptor
FF	0.933	1.347	open	weak σ-donor, π-donor
FH	0.917	1.355	open	weak σ-donor, π-donor
OC	0.911	1.352	open	weak σ-donor, π-donor
CH_2 ($^1A_1$)	0.901	1.333	open	σ-donor
NH_3	0.894	1.337	open	σ-donor
OH_2	0.866	1.294	ring	σ-donor, π-donor

Table VIII. Comparison of the Bond Orders n of the CX Bond in CH_2X^{2+} (Type I) and $CH_2X(H_2)^{2+}$ (Type III) Dications

X	bond order n	
	I	III
FH[a]	<1	≪1
OC	0.97	0.72
NN	0.94	0.75
OH_2	1.19	0.89
NH_3	1.20	0.94
CO	1.25	1.22
CH_2 ($^1A_1$)	1.84	1.46

[a] ρ_b = 1.423 (I) and 1.080 e/Å^3 (III).

In the following we discuss the influence of X on the interactions between CH_2^{2+} and H_2. It is easy to see that these interactions depend strongly (i) on the electron population of the pπ(C) orbital in CH_2X^{2+} and (ii) on the total charge at C and the resultant *effective* electronegativity of C. Both (i) and (ii) in turn depend on the σ/π-donor ability of X.

In Table VII relevant information on the structure of type III dications in dependence on the nature of X is summarized. If X is both a σ/π-donor and a π-acceptor (because of a low-lying π^* MO) as in the case of X = CO and N_2, then the π-acceptor ability of X causes electron withdrawal from H_2 (Figure 8b). π-donation from a filled $\pi(X)$ MO into the pseudo-π MO (Figure 8b) leads to (i) weakening of the C-H bonds of the CH_2^{2+} acceptor and (ii) strengthening of the H_2C-Y_2 bonds (Figure 8b). In the case of X = CO, all four C-H bonds are now equal (Table VII).[36]

If X = OH_2, then the σ- and π-donor ability of X will largely prevent σ-withdrawal from H_2. However, at the same time C,H

(36) In ref 7d, a C_s structure was reported as minimum for CH_4CO^{2+}. However, we found our structure **32** to be the only CH_4X^{2+} species where a C_{4v} geometry was lower in energy than the corresponding C_s geometry.

interactions are established via the pseudo-π MO (Figure 8b). As a consequence, a three-membered ring structure is found (compare with Figure 7). The H–H and C–H bond paths are strongly curved inward, indicating that all ring bonds are weak.[26] Relatively small electronic changes will lead to either the open or the T structure of the donor–acceptor complex.

A comparison of the C–X bond properties of type III dications with those found for type I dications (Table VIII) is helpful when assessing the actual donor ability of X in the presence of H_2 as the second donor. In all cases considered the bond order n is decreased in type III complexes, indicative of a reduced donor activity of X. The decrease in the bond order is smallest for CO and largest for OH_2.

The stabilization due to electron donation from X in type III dications can be determined by calculating the reaction energies ΔE_R for reaction 2.

$$CH_4^{2+} + X \rightarrow CH_4X^{2+} + \Delta E_R \qquad (2)$$

The calculated results shown in Table II support the conclusion that the donor selectivity of X is reduced in type III complexes compared to type I dications. In all cases the ΔE_R values are smaller for reaction 2 than for reaction 1. However, the relative donor ability is nearly the same and comparable to the order of proton affinities. The following sequence is found for reaction 2:

$$CH_2 > NH_3 > OH_2 > CO \sim CH_4 > N_2 > FH > H_2 \sim OC > F_2$$

Contrary to type I dications, a lone-pair donor structure with $X = F_2$ could be located (**35**) for CH_4X^{2+}. The computed relatively small ΔE_R value for **35** in reaction 2 is in agreement with the calculated low proton affinity of F_2.

The correlation of the eigenvalues ϵ_{HOMO} of X with ΔE_R of reaction 2 is shown in Figure 3. The donor–acceptor interaction is clearly a function of the frontier orbital energy levels. The lower lying LUMO of CH_2^{2+} ($\epsilon_{LUMO} = -19.25$ eV) also explains the larger interaction in Type I dications compared to CH_4X^2 structures ($\epsilon_{LUMO}(CH_4^{2+}) = -16.48$ eV).

The optimized geometries of **28–36** are in agreement with the argumentation presented here. All C–X bonds are longer compared to the respective type I dication. The bond lengthening in X resulting from donor–acceptor interaction is less pronounced, and besides CO N_2 also now has a shorter bond compared to the isolated molecule. Due to distortion from local C_{4v} symmetry of the CH_4 unit, CH_4AB^{2+} structures deviate more or less from linearity in C–A–B (with the exception, of course, of AB = CO), and $X = OH_2$ is found with a nonplanar arrangement.

(5) Comparison of Different Types of Dications. The results discussed above may now be combined to produce a detailed picture of the ability of donors X in type I dications to allow for additional electron donation by H_2 resulting in type III dications, since the latter may be considered as hydrogenated type I complexes. Intuitively, the extend of H_2 donation might be anticipated to be a function of the "hole" left by X donation (and vice versa), and additivity of stabilization should be found. The discussion in the previous section indicated already that this is not the case. The stabilization due to H_2 charge donation may be calculated via reaction 3.

$$CH_2X^{2+} + H_2 \rightarrow CH_2X(H_2)^{2+} + \Delta E_R \qquad (3)$$

The calculated values of ΔE_R are listed in Table II. To simplify the discussion, only the hydrogenation of type I dications **20–26** leading to type III dications **28–34** shall be considered. The E_R values for reaction 3 establish the following order:

$$CO > FH > N_2 > OC > CH_2 > NH_3 > OH_2$$

The amount of charge donation from H_2 can also be related to the H–H atomic distances in **28–34**. The following sequence is found (Table VII):

$$CO > N_2 > FH > OC > CH_2 > NH_3 > OH_2$$

Both sequences are nearly identical and demonstrate that the stabilization which can be expected from interaction of type I dications CH_2X^{2+} with a second donor Y_2 is not simply a function of the donor strength of X. It rather depends on the strength of the actual type of orbital interaction as discussed above.

Chart II. $C_6H_6^{2+}$ Structures A, B, and C Taken from Reference 9

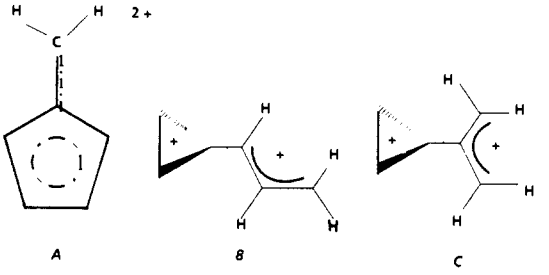

While for $CH_4F_2^{2+}$ a structure (**35**) could be located as minimum with F_2 as the lone-pair donor, this was not possible for $CH_2F_2^{2+}$. The presence of H_2 as a second donor for $CH_2F_2^{2+}$ reduces π-donation from X in type III dications (Figures 8) and stabilizes **35** sufficiently to become a minimum on the potential energy hypersurface. However, a prediction which can be made based on the discussion of type II and type III dications is that there must be a more stable isomer of $CH_4F_2^{2+}$ than structure **35**. Since F_2 is a better σ than lone-pair donor, this structure should correspond to a doubly hydrogenated CF_2^{2+}, similar to structure **36** (Chart I) with two fluorine atoms instead of (nonbridged) hydrogen. After this study was completed, a C_{2v} structure for $CH_4F_2^{2+}$ corresponding to **36** was calculated and found to be 56.4 kcal/mol lower in energy than **35**.[37] This leads now to a negative hydrogenation energy of −23.8 kcal/mol for reaction 3 (Table II).[37]

IV. Summary and Outlook

The geometries and stabilities of dications can in many cases be rationalized by the donor and acceptor strength of constituting subunits. In this way the existence of unusual structures such as CH_2X^{2+} **20–27** and CH_4X^{2+} **28–37**, which are unknown or very unstable as neutral molecules, finds a logical explanation. The detailed examination of the geometries and bonding features of the dications investigated here leads to three different classes of dications which are distinguished by the type and number of donor–acceptor interaction. The simple donor–acceptor model presented here may be used to predict unknown dications or to explain results of experiments or quantum chemical calculations. To illustrate this, two examples taken from the literature shall shortly be discussed.

In a combined experimental and theoretical investigation, Koch et al.[38] reported that the global minimum of CH_3O^{2+} corresponds to the oxoniomethylene dication $HC{-}OH_2^{2+}$ (A). It was found to be 22.7 kcal/mol lower in energy than the second minimum, the hydroxymethyl dication $H_2C{-}OH^{2+}$ (B). A third structure, the methoxy dication $H_3C{-}O^{2+}$ (C), is 116.8 kcal/mol higher in energy than A. Could this result be predicted with use of the donor–acceptor model for CH_3O^{2+}? The answer is yes. A, B, and C can be considered as donor–acceptor complexes arising from acceptors CH^{2+}, CH_2^{2+}, and CH_3^{2+} and donors OH_2, OH, and O. The frontier orbitals establish a sequence of donor strength $OH_2 > OH > O$, and the acceptor strength is found as $CH^{2+} > CH_2^{2+} > CH_3^{2+}$.[39] Thus, the stability order is in perfect

(37) E(tot) at MP3/6-31G*//6-31G* for this isomer of $CH_4F_2^{2+}$ is −238.3723 hartrees: Frenking, G.; Koch, W., unpublished result.

(38) Koch, W.; Maquin, F.; Schwarz, H.; Stahl, D. *J. Am. Chem. Soc.* **1985**, *107*, 2256.

(39) At 6-31G*/6-31G*, the eigenvalues ϵ_{HOMO} of OH_2, OH, and O (^1D) are the following: −13.56, −13.72, −15.67 eV. At the same level of theory, the eigenvalues ϵ_{LUMO} of CH^{2+}, CH_2^{2+}, and CH_3^{2+} are the following: −21.74, −19.25, −19.51 eV. The geometries were taken from ref 33. For CH^{2+}, the geometry of CH^+ was taken.

(40) Klopman, G., Ed. *Chemical Reactivity and Reaction Paths*; Wiley: New York, 1973.

(41) Aue, D. H.; Bowers, M. T. In *Gas-Phase Ion Chemistry*; Bowers, M. T., Ed.; Academic Press: New York, 1979; Vol. II.

agreement with the strength of the donor–acceptor interaction indicated by the frontier orbitals.

The second example concerns energetically low-lying structures of $C_6H_6^{2+}$ as reported in a theoretical investigation by Lammertsma and Schleyer.[9] The number of possible isomers is very high, and a qualitative model to predict stable structures will aid the search. As noted before, analogy to neutral isomers is no help. Thirteen structures are reported, and three (A, B, C) were found to be candidates for the global minimum.

Again, this could have been predicted on the basis of our model. In our study we found the strongest bonding between CH_2^{2+} as acceptor and CH_2 ($^1A_1$) as donor. All three low-lying $C_6H_6^{2+}$ isomers A, B, and C correspond formally to donor–acceptor complexes between CR_2^{2+} and singlet carbenes. In case of A, planarity is found due to stronger π-conjugation relative to hyperconjugation.[42]

One referee argued that, based on our model, more stable structures should be expected with CR^{2+} as donor rather than CR_2^{2+}. In fact, one of the 13 isomers for $C_6H_6^{2+}$ reported in ref 9 represents a donor–acceptor complex between CH^{2+} and C_5H_5, but it is much higher in energy compared to A, B, or C. This can be explained by the very unfavorable overlap between donor and acceptor unit in this structure which forms a pyramidal geometry with an apical CH^{2+} acceptor and basal C_5H_5 donor.[9] It seems that no suitable donor unit for C_5H_5 can be formed which can interact in a favorable way with CH^{2+}. In this context it is interesting to learn that in the meantime the same 13 structures have been calculated for the triply charged $C_6H_6^{3+}$ isomers.[45] Again, structures A, B, and C were found as energetically lowest lying species, but the stability differences were found to be larger at the same level of theory.[45] It seems that the differences in donor–acceptor interaction become more pronounced in higher charged species.

Our analysis of donor–acceptor interaction does not cover all kinds of possible orbital interaction. For example, stable structures may arise from donor–acceptor interaction involving π-donors. Hexacoordinated pyramidal carbodications, a well-known class of cations which is even stable in solution,[2,11] can be explained by the interaction between an apical RC^{2+} acceptor and a basal π-donor. Thus, the model of donor–acceptor interaction may still be extended.[46]

It is more the rule than the exception that the structure of a doubly charged species is substantially different compared to the respective neutral molecule. The simple model presented here is of great value for predicting structures of stable dications.

Acknowledgment. This work has financially been supported by the Fonds der Chemischen Industrie. G.F. thanks Dr. Jack Collins for stimulating discussions and constructive criticism on a preliminary version of the manuscript. D.C. thanks the Deutsche Forschungsgemeinschaft and the Rechenzentrum der Universität Köln for support. W.K. thanks Nikolaus Heinrich for helpful discussions.

(42) For a discussion and further examples of planar, substituted ethylene dications see ref 35.

(43) This is a qualitative approach to demonstrate the basic principle. A more detailed account of frontier orbital interaction has to consider orbital coefficients. For example, the different reaction energies when CO donates electronic charge via oxygen or carbon may be explained by the larger coefficient at carbon for the lone-pair HOMO. For further discussion of frontier orbital interaction, see ref 21.

(44) The total energy of CF_2^{2+} at MP3/6-31G*//6-31G* is -235.9412 hartrees. The geometry was taken from the following: Koch, W.; Frenking, G. *Chem. Phys. Lett.* **1985**, *114*, 178.

(45) Koch, W.; Schwarz, H. *Chem. Phys. Lett.* **1985**, *113*, 145. A different analysis has been given by the following: Jemmis, E. D.; Schleyer, P. v. R. *J. Am. Chem. Soc.* **1982**, *104*, 4781.

(46) A different analysis has been given by the following: Jemmis, E. D.; Schleyer, P.v.R. *J. Am. Chem. Soc.* **1982**, *104*, 4781.

Barriers to Rotation Adjacent to Double Bonds. 2. *n*-Propyl vs. Isopropyl Groups

Kenneth B. Wiberg

Contribution from the Department of Chemistry, Yale University, New Haven, Connecticut 06511. *Received March 28, 1986*

Abstract: The barriers to rotation about the C–C bonds adjacent to the carbonyl groups of isobutyraldehyde, methyl isopropyl ketone, and isobutyric acid were calculated. The 3-21G basis set was used for the geometry optimizations, and the 6-31G* basis set was used to obtain the energies. The differences in energy between R = *n*-propyl and isopropyl also were calculated and reproduced the observed energy differences. Whereas the more branched isomer had a significantly lower energy for the aldehydes and acids, the difference in energy was very small with the ketones. The components of the barrier are discussed. The traditional decomposition into 1-, 2-, and 3-fold terms does not provide a useful representation of the interactions which are involved. Besides the 3-fold barrier observed with compounds having R = CH_3, the major contributions to the barrier arise from the stabilizing interaction between an alkyl group and the carbonyl ($\sim$1 kcal/mol) and from the repulsive interaction between one of the methyls of the isopropyl group and the other substituent at the carbonyl. A hydroxy group (i.e., in a carboxylic acid) leads to a significantly smaller steric interaction than found with a methyl group (i.e., in a methyl alkyl ketone).

The conformations of ketones have been of considerable interest in connection with studies of stereoselection in addition to the carbonyl group. Models for the addition have been developed by Cram,[1] ,Cornforth,[2] Karabatsos,[3] Felkin,[4] and others.[5] Theoretical studies of the activated complexes for addition to carbonyl groups by Ruch and Ugi,[6] Salem,[7] and especially Anh and Eisenstein[8]

(1) Cram, D. J.; Abd Elhafex, F. A. *J. Am. Chem. Soc.* **1952**, *74*, 5828.

(2) Cornforth, J. W.; Cornforth, R. H.; Mathew, K. K. *J. Chem. Soc.* **1959**, 112.

(3) Karabatsos, G. J. *J. Am. Chem. Soc.* **1967**, *89*, 1367.

(4) Cherest, M.; Felkin, H.; Prudent, N. *Tetrahedron Lett.* **1968**, 2201. Cherest, M.; Felkin, H. *Ibid.* **1968**, 2205.

(5) For a summary of previous studies, see: Wipke, W. T.; Gund, P. *J. Am. Chem. Soc.* **1976**, *98*, 8107.

(6) Ruch, E.; Ugi, I. *Top Stereochem.* **1969**, *4*, 99.

0002-7863/86/1508-5817$01.50/0